Giftet Inc.
Journal of Geolocation, Geo-information, and Geo-intelligence
Volume 2020, article ID 2020071605, 9 pages
https://doi.org/10.18610/JG3.2020.071605

Technical Report

An Underground System of Stationary Pseudolites

Ilir F. Progri[1] and William R. Michalson[2]

[1]*Giftet Inc., 5 Euclid Ave. #3, Worcester, MA 01610, USA*

[2]*Electrical and Computer Engineering Department, Worcester Polytechnic Institute, Worcester, MA 01609, USA*

ORCID: 0000-0001-5197-1278

Correspondence should be addressed to Ilir Progri; iprogri@giftet.com.

Received June 7, 2020; Revised June 8, 2020-July 10, 2020, Accepted July 16, 2020; Published November 1, 2020.

Editor-in-Chief/Scientific Editor: Ilir F. Progri

Abstract—By placing pseudolites[i] at strategic locations in underground locations such as tunnels, it becomes possible to maintain navigation capabilities in situations where signals from the GPS system are unavailable. By knowing the precise location of the pseudolites, and by having one antenna on a vehicle and another fixed in the tunnel, it is possible to quickly resolve ambiguities and achieve high accuracy. The achievable accuracies using such a system are presented in this paper.

Index Terms—Pseudorange, Doppler, accumulated carrier phase, measurements, navigation, pseudolites, Kalman, least square algorithm, ionospheric propagation delay, indoor terrestrial applications.

1 Introduction

In early 2000, the Global Positioning System (GPS) experienced significant improvements due the removal of the Selective Availability (SA). Despite this improvement, the GPS still cannot be used when obstacles prevent the receiver from acquiring at least a minimum number of GPS satellites (four is three-dimensional positioning and local time is needed). The most severe of these situations is when navigation is needed in areas where there is significant blockage of the GPS as occurs within cannons or tunnels. In these situations, reliable tracking of the GPS signal is impossible.

To provide navigation in these situations it is necessary to augment the GPS. One such augmentation is to provide additional GPS-like signals from ground-mounted pseudolites. This basic idea has been explored and analyzed by a number of researchers in USA and abroad [1]-[8]. This idea presents a quite natural blending of the processing of the GPS satellite signals with the GPS pseudolite signals. Briefly, we will mention some of the benefits of using the GPS pseudolites:

1. Pseudolites can be placed at arbitrary locations on the ground.
2. The transmitted frequency can be selected for the particular situation.
3. Low cost allows using several pseudolites in an overall system design.
4. The signal strength can be customized.

By exploiting these characteristics, a tremendous improvement in navigation system accuracy can be achieved. However, despite this benefit, such a system also has limitations:

1. The terrain geometry can impose limits on the location of the pseudolites.

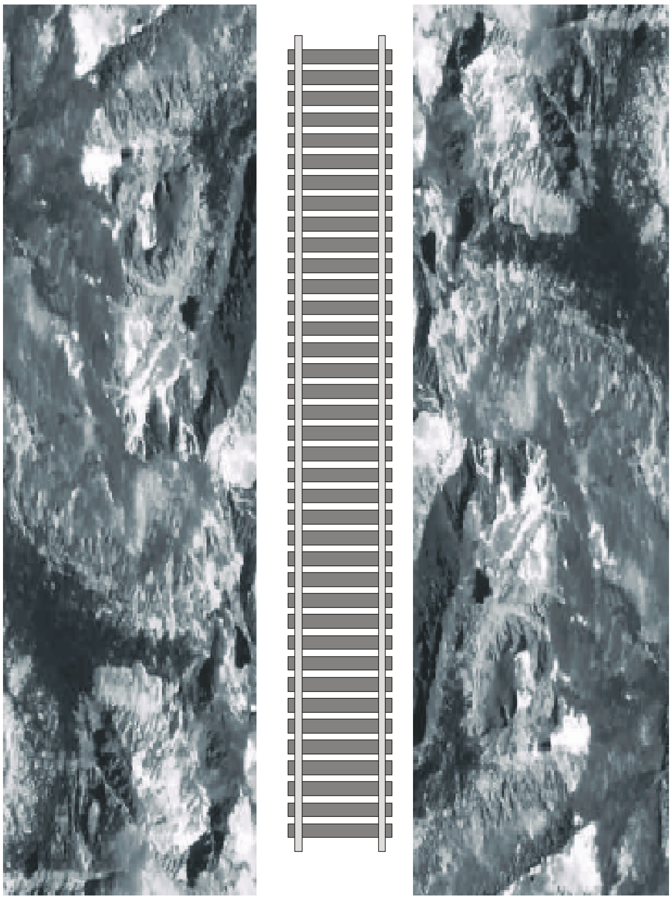

Fig. 1. Straight tunnel description.

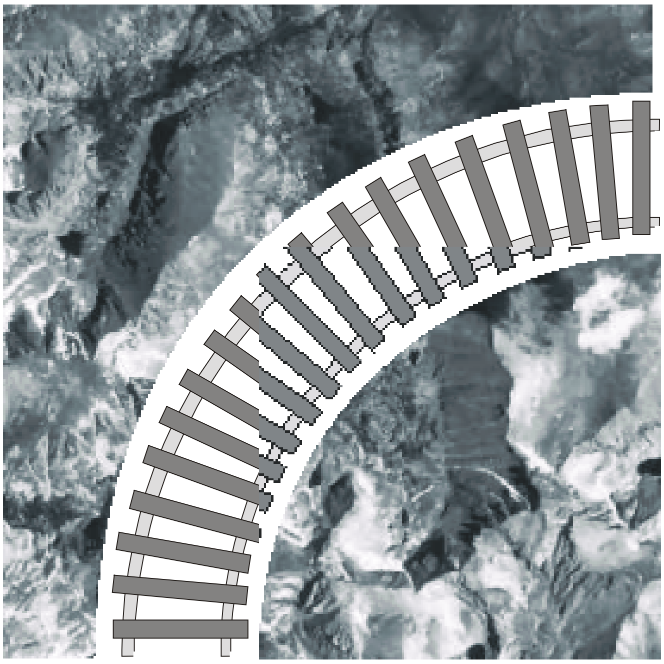

Fig. 2. Curved tunnel profile.

2. There are physical bounds on the transmitted frequency.
3. The number of pseudolites is directly linked with the overall cost of the system.
4. The potentially close proximity between a receiver and the pseudolites can require receivers with very high dynamic range (the near-far problem).

Therefore, in order to achieve centimeter level position accuracy and centimeter/sec level velocity accuracy a very careful selection of system parameters is required. This selection forms the first part of the main theme of this research; the second part is the actual design of the system.

This paper is organized as follows: In Sect. 2 we discuss an underground pseudolite system description. The simulation of a simplified underground pseudolite indoor geolocation system is provided in Sect. 3. Conclusion is summarized in Sect. 4 followed by acknowledgment in Sect. 5 and references in Sect. 6.

2 Underground Pseudolite System Description

Consider a tunnel as the most severe example of an underground obstacle that is used for trains, subways, cars, boats, pedestrians, etc.

In any of these environments the acquisition or tracking of a GPS or GNSS signal is either unavailable or unreliable. If the GNSS signal is unavailable then the GNSS solution is either used from the most recent solution. If the GNSS signal is unreliable that means that the GNSS signal will fail the integrity test [4], [9], [10], [16], [18] and hence the solution of the GNSS signal is erroneous and it cannot be used. Therefore, other means of navigation must be used to enable a real-time solution of the position, navigation, and timing (PNT), position, velocity, and timing (PVT) in any of these environments.

An underground system of stationary pseudolites or an indoor (underground) geolocation system may be used to provide reliable PNT and PVT information.

In this paper considers a simplified the signal model description. Detailed descriptions of RF signal description, modulation, demodulation, processing is subject of other publications [22], [24]. The main purpose of this paper is to preserve the initial technical merits or the preliminary analysis of this work that was completed some twenty years earlier. The technical shortcomings of this paper will be filled in future publications.

The geometry of a typical tunnel is pictured in Figs. 1 and 2. Figure 1 depicts a top cutaway[ii] (or the cross section cut of the profile) view of a straight tunnel.

Similarly, Fig. 2 depicts a curved tunnel. It is easy to visualize that any tunnel can be formed as a combination of the

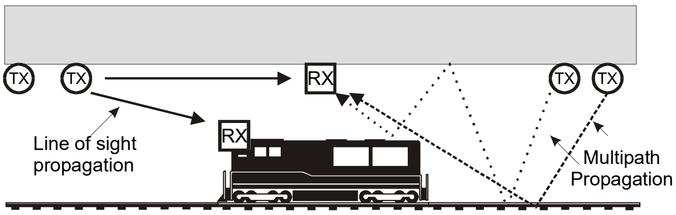

Fig. 3. LOS paths with single/multiple reflection paths.

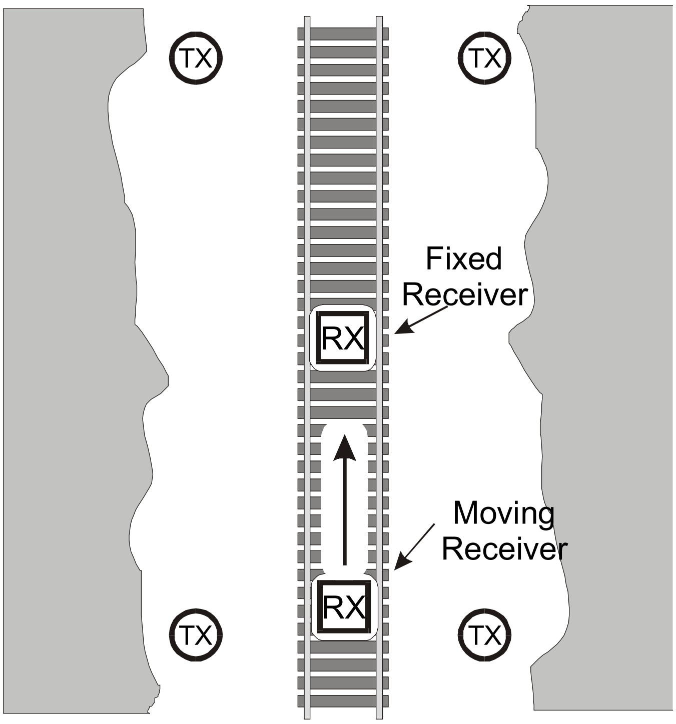

Fig. 4. An underground system of stationary pseudolites description.

two tunnels given in Figs. 1 and 2.

Figure 3 illustrates the navigation system being proposed. The pseudolite transmitters are denoted as TX and the receivers are denoted as RX. Space limitations between tunnel walls and the train restricts the TX and RX locations.

For curved tunnels the line of sight will continually change thus limiting the visibility of pseudolites and receivers. Therefore, the location of equipment is tunnel dependent.

In this system, the tunnel walls and the train serve as reflective surfaces, thus increasing the effect of multipath on the navigation solution. Under the assumption that the pseudolite signal is a spread spectrum signal of 20 MHz-bandwidth, selecting the pseudolite center frequencies such that any pair has a non-overlapping spectrum can eliminate interference of one signal with another. Hence, the total effect of multipath is reduced to minimum. Although this solution is possible, we attempt to maintain the same pseudolite center frequency and approach elimination of the multipath effect by different means.

2.1 *Underground Multipath Model*

Given that the multipath is the most severe error source, it is important to model and analyze it correctly. This analysis shows the effect of multipath on pseudorange, accumulated carrier phase, and Doppler measurements.

Assume that a signal transmitted from a point with coordinates $A(\boldsymbol{r},t)$, can be modeled as,

$$s(t) = S(t)e^{j\phi}\delta(t) \quad (1)$$

Where

$S(t)$ denotes the amplitude of the transmitted signal,

ϕ denotes the total phase of the transmitted signal as seen in point $A(\boldsymbol{r},t)$,

Assuming a wide band signal with infinite bandwidth, we represent it in time domain with the help of the Dirac delta function, $\delta(t)$,

$$r(t) = R(t)e^{j(\phi-\theta)}\delta(t-\tau) \quad (2)$$

The unknown quantities of (2) are explained below,

$R(t)$ denotes the received signal amplitude;

θ denotes the phase change of the received signal while traveling from point A to point B;

τ represents the delay of the received signal.

Neglecting clock effects (both bias and drift) for simplicity we can determine the range between A and B assigned by $d_{A\leftrightarrow B}$. Assuming that the signal travels at speed c with center frequency f, the phase change of the received signal is obtained from,

$$\theta = 2\pi f(d_{A\leftrightarrow B}/c \equiv \tau) \quad (3)$$

The pseudorange measurements are directly linked with the distance $d_{A\leftrightarrow B}$, the carrier phase measurements are directly linked with the phase changed of the received signal plus an unknown integer, and Doppler measurements are directly linked with delay of the received signal θ. We should also mention that the amplitude of the received signal relates to the amplitude of the transmitted signal as follows:

$$R(t) = A(t)/d_{A\leftrightarrow B} \quad (4)$$

Assume now that the received signal is coming from more than one path (including the LOS path see Fig. 3) and denote by M the total number of paths that the signal goes through from point A to B[iii]. If the path has been reflected $[M_i]$ times before arriving at the receiver, and at each reflection the reflection coefficient is a_{ij}, the overall reflection factor is

$$a_i = \prod_{j=1}^{M} a_{ij} \quad (5)$$

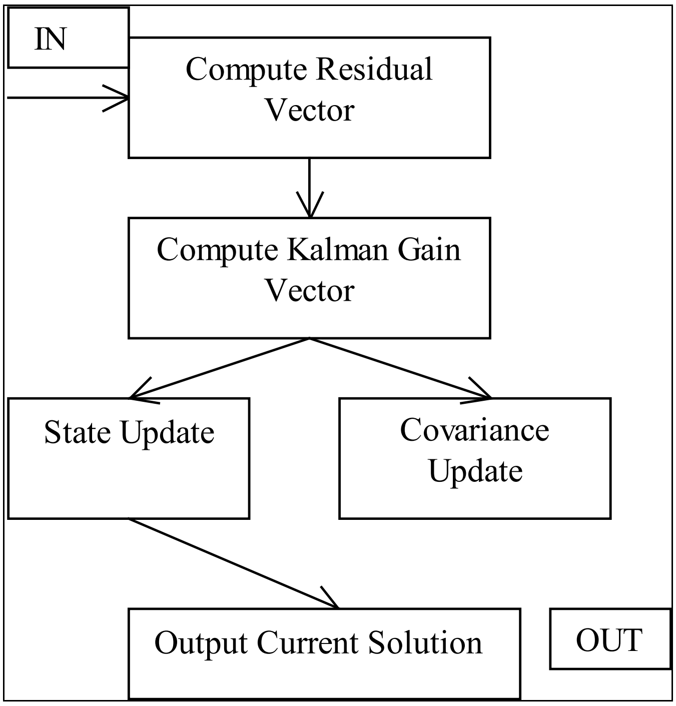

Fig. 5. Kalman filter state update.

It to see that for the LOS path the reflection coefficient is $+1$. Therefore, the analytical expression for the received signal arriving from M paths is,

$$r(t) = e^{j\phi}\left[\frac{R(t)\delta(t-\tau)}{e^{j\theta}} = A(t)\sum_{i=1}^{M}\frac{a_i}{d_i}\frac{\delta(t-\tau_i)}{e^{j\theta_i}}\right] \quad (6)$$

The result of expression (6) can be written as

$$R(t) = A(t)\frac{1}{d} = A(t)\sum_{i=1}^{M}\frac{a_i}{d_i} \quad (7)$$

where d is the equivalent LOS distance of the signal determined from,

$$\frac{1}{d} = \sum_{i=1}^{M}\frac{a_i}{d_i} \text{ or } d = \frac{1}{\sum_{i=1}^{M}\frac{a_i}{d_i}} \quad (8)$$

We can now easily determine the effect on Doppler and the accumulated phase by referring to (3),

$$\tau = d/c \text{ and } \theta = 2\pi f(\tau \equiv d/c) \quad (9)$$

The result obtained in (7)-(9) enables us to rewrite the received signal at point B as,

$$r(t) = R(t)e^{j(\phi-\theta)}\delta(t-\tau) \quad (10)$$

The error in the pseudorange, accumulated carrier phase, and Doppler measurements due to the presence of multipath are defined by

$$\varepsilon_{\rho}^{M} = d - d_{A\leftrightarrow B} \text{ (m)} \quad (11)$$

$$\varepsilon_{\phi}^{M} = 2\pi f(d - d_{A\leftrightarrow B})/c, \text{ (rad) or, } \varepsilon_{\phi}^{M} = d - d_{A\leftrightarrow B} \text{ (m)} \quad (12)$$

$$\varepsilon_{\dot\phi}^{M} = (d - d_{A\leftrightarrow B})/c \text{ (sec) or } \varepsilon_{\dot\phi}^{M} = \dot d - \dot d_{A\leftrightarrow B} \text{ (m/sec).} \quad (13)$$

The superscript M denotes "due to multipath." The subscript ρ, φ, and $\dot\varphi$, denote relationship with pseudorange, carrier phase, and Doppler respectively. The single dot on top of a variable describes the first derivative with respect to time.

For simulation purposes, we will assume that d_i are gamma distributed from $[d_{A\leftrightarrow B}, \infty)$ and that the reflection coefficient are uniformly distributed from $[0,1]$ [20].

2.2 Proposed Underground System of Stationary Pseudolites

In the previous analysis we showed that multipath is dependent on the geometry of the tunnel as well as the reflection coefficient, which to a large extent depends on the surface and the surface material. If the tunnel surface is made of the same material and has a uniform reflection coefficient, the multipath inside the tunnel will be largely dependent on the tunnel geometry. Therefore, the main theme in this subsection is to come up with a system design uses the geometry as the key element to eliminate the undesired effect of multipath.

The intent is to perform accumulated carrier phase processing, because the carrier phase measurement error is the smallest of the measurement errors in the receiver [17], [21].

Rewrite the analytical formulation of the carrier phase measurement between the f^{th} (fixed) receiver and the j^{th} pseudolite, $\phi_f^j[k]$, as follows,

$$\phi_f^j[k] = \left|\begin{array}{l} d_f^j[k] + c\left(\Delta t_f[k] - \Delta t^j[k]\right) + \lambda a_f^j[0] \\ +\varepsilon_{j\phi}^{M}[k] + \varepsilon_f^{\phi}[k] \end{array}\right. \quad (14)$$

where

$d_f^j[k]$ denotes the geometric distance between the f^{th} receiver and the j^{th} pseudolite;

$\Delta t_f[k]$ denotes the f^{th} receiver clock bias;

$\Delta t^j[k]$ similarly determines the j^{th} pseudolite clock bias;

$a_f^j[0]$ represents the number of unknown cycles between the f^{th} receiver and the j^{th} pseudolite at the initial moment of tracking;

$\varepsilon_{j\varphi}^{M}[k]$ depicts the multipath error (see (12)) of receiving the signal from the j^{th} pseudolite from paths different from the LOS path;

$\varepsilon_f^{\varphi}[k]$ denotes the carrier phase measurement error of the f^{th} receiver;

k is the epoch index from the moment of tracking the carrier

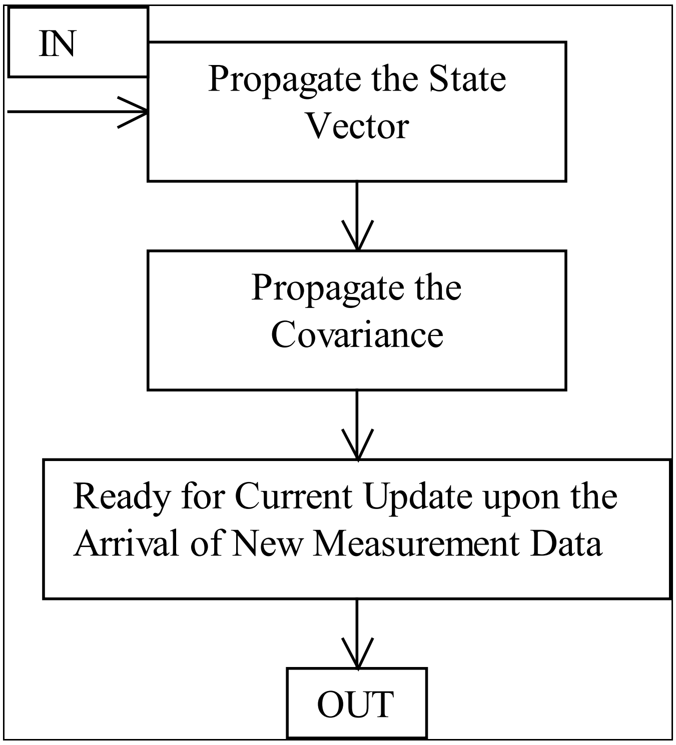

Fig. 6. Kalman filter state propagation.

phase of the j^{th} pseudolite;

$\lambda = c/f$ is also known as the wavelength of the carrier phase.

Assume that the l^{th} pseudolite is symmetrically positioned between receiver f^{th} and the j^{th} pseudolite as shown in Fig. 4. Also assume there is another receiver which is stationary on the locomotive or which moves relative to the stationary receiver. The expression for the carrier phase between the l^{th} pseudolite and the m^{th} (moving) receiver reads,

$$\phi_m^l[k] = \left| \begin{array}{l} d_m^l[k] + c(\Delta t_m[k] - \Delta t^l[k]) + \lambda a_m^l[0] \\ +\varepsilon_{l\varphi}^M[k] + \varepsilon_m^\phi[k] \end{array} \right. \tag{15}$$

A similar expression can be formulated for the accumulated carrier phase between the l^{th} pseudolite and the i^{th} receiver and phase between the j^{th} pseudolite and the m^{th} receiver as follows,

$$\phi_i^l[k] = \left| \begin{array}{l} d_i^l[k] + c(\Delta t_i[k] - \Delta t^l[k]) + \lambda a_i^l[0] \\ +\varepsilon_{l\phi}^M[k] + \varepsilon_i^\phi[k] \end{array} \right. \tag{16}$$

$$\phi_m^j[k] = \left| \begin{array}{l} d_m^j[k] + c(\Delta t_m[k] - \Delta t^j[k]) + \lambda a_m^j[0] \\ +\varepsilon_{j\phi}^M[k] + \varepsilon_m^\phi[k] \end{array} \right. \tag{17}$$

First, we form the difference between (14) and (16) and between (15) and (17) to obtain two independent quantities,

$$\phi_i^{j-l}[k] = \left| \begin{array}{l} d_i^{j-l}[k] + c\Delta t^{j-l}[k] + \lambda a_i^{j-l}[0] + \\ \varepsilon_{(j-l)\phi}^M[k] + 2\varepsilon_i^\phi[k] \end{array} \right. \tag{18}$$

$$\phi_m^{j-l}[k] = \left| \begin{array}{l} d_m^{j-l}[k] + c\Delta t^{j-l}[k] + \lambda a_m^{j-l}[0] \\ +\varepsilon_{(j-l)\phi}^M[k] + 2\varepsilon_m^\phi[k] \end{array} \right. \tag{19}$$

Under the assumption that the i^{th} and j^{th} pseudolites are symmetrically positioned, the i^{th} and m^{th} receiver yields elimination of the single difference multipath error or,

$$\varepsilon_{(j-l)\phi}^M[k] \cong 0 \tag{20}$$

Now we form the double difference quantity as,

$$\phi_{m-i}^{j-l}[k] = d_{m-i}^{j-l}[k] + \lambda a_{m-i}^{j-l}[0] + 2\left(\varepsilon_i^\phi[k] + \varepsilon_m^\phi[k]\right) \tag{21}$$

Assume that both the moving receiver and the fixed receiver are identical; i.e., the standard deviation on the carrier phase measurement error is the same for either receiver. This produces,

$$\phi_{m-i}^{j-l}[k] = d_{m-i}^{j-l}[k] + \lambda a_{m-i}^{j-l}[0] + 4\varepsilon_\phi[k] \tag{22}$$

Let L be the number of pairs of pseudolites, positioned almost symmetrically (see endnote iii) on both sides of the multipath axis of symmetry as shown in Fig. 4. We can write (22) in vector/matrix notation as,

$$\mathbf{\Phi}[k] = \mathbf{d}[k] + \lambda\mathbf{a}[0] + 4\mathbf{e}[k] \tag{23}$$

Therefore, assuming that the filter states are the position, velocity, acceleration of the moving vehicle and double difference ambiguities we obtain the following measurement (observable) vector/matrix equation,

$$\mathbf{\Phi}[k] \cong \mathbf{H}[k]\mathbf{s}[k] + 4\mathbf{e}[k] \tag{24}$$

Where, $\mathbf{H}[k]$ denotes the measurement matrix which relates the state vector with the observable vector of the double difference accumulated carrier phase. Utilizing a Kalman filter to describe the system dynamics; thus, for a transition matrix $\mathbf{T}[k]$ the propagation state vector is formulated with the help of the following expression [21],

$$\mathbf{s}[k+1] = \mathbf{T}[k]\mathbf{s}[k] + \mathbf{w}[k] \tag{25}$$

The process noise $\mathbf{w}[k]$ is assumed white sequence with known covariance $\mathbf{Q}[k]$ and uncorrelated with double carrier phase measurement noise, $\mathbf{R}[k]$.

Eliminating the intermediate steps, we present here the final solution of the Kalman (recursive) filter in two major phases,

2.3 Kalman Filter State Update

We seek to update the state (see Fig. 5) in accordance with

$$\hat{\mathbf{s}}[k] = \hat{\mathbf{s}}[k]^- + \mathbf{G}[k](\mathbf{\Phi}[k] - \mathbf{H}[k]\hat{\mathbf{s}}[k]^- \equiv \mathbf{z}[k]) \tag{26}$$

In (26), $\hat{\mathbf{s}}[k]^-$ represents the state vector in the *a priori* estimate, $\mathbf{z}[k]$ is defined as the residual vector; and the matrix G[k] denotes the Kalman gain matrix which in its optimal form

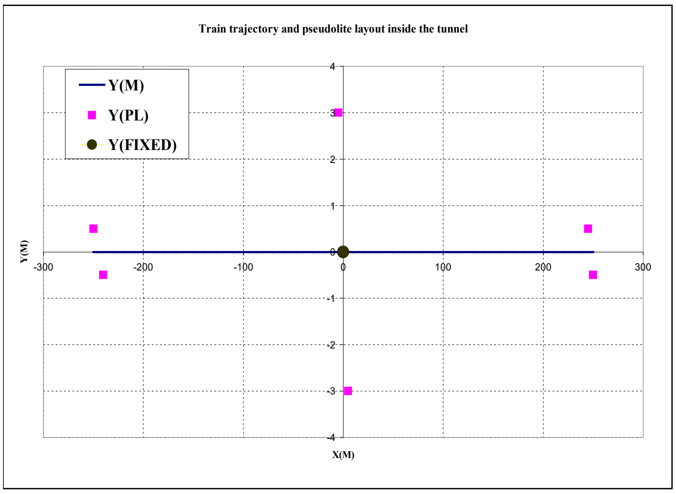

Fig. 7. Train trajectory and pseudolite layout inside the tunnel.

is written as,

$$\mathbf{G}[k] = \mathbf{C}[k]^{-}\mathbf{H}[k]^{\dagger}(\mathbf{H}[k]\mathbf{C}[k]^{-}\mathbf{H}[k]^{\dagger} + \mathbf{R}[k])^{-1} \quad (27)$$

where superscript † denotes the matrix transpose operator.

The update equations for the covariance matrix $\mathbf{C}[k]$ in its sub-optimal and optimal form are

$$\mathbf{C}[k] = \begin{cases}(\mathbf{I} - \mathbf{G}[k]\mathbf{H}[k])\mathbf{C}[k]^{-}(\mathbf{I} - \mathbf{G}[k]\mathbf{H}[k])^{\dagger} \\ +\mathbf{G}[k]\mathbf{R}[k]\mathbf{G}[k]^{\dagger}\end{cases} \quad (28)$$

$$\mathbf{C}[k] = (\mathbf{I} - \mathbf{G}[k]\mathbf{H}[k])\mathbf{C}[k]^{-} \quad (29)$$

Equations (26) through (29) form the heart of the Kalman filter state update phase. State update is followed by state propagation also known as the time update or time propagation phase,

2.4 Time Update or State, Time Propagation

One equation of the state or time propagation vector (see Fig. 6) is obtained by modifying (25),

$$\hat{\mathbf{s}}[k+1]^{-} = \mathbf{T}[k]\hat{\mathbf{s}}[k] \quad (30)$$

The state error covariance matrix (see Fig. 6) changes in accordance with,

$$\mathbf{C}[k+1]^{-} = \mathbf{T}[k]\mathbf{C}[k]\mathbf{T}[k]^{T} + \mathbf{Q}[k] \quad (31)$$

This concludes the discussion on the time update or the state, time propagation.

3 Simulation

The simulation section consists of a simplified underground pseudolite system and the assessment of simulation results.

3.1 A Simplified Underground Pseudolite System

A generic train trajectory inside the tunnel is depicted in Fig. 7. This trajectory was generated very simply as follows: it is assumed that the train moves along the x (north) axis of a local coordinate system (using a North, East, Down coordinate frame) with a velocity along this axis of 10 m/s (36 km/h); it is further assumed that receiver sits on top of the train (locomotive) on an altitude of 5 m from the ground. The velocity components along the y (east) and z (down) are zero m/sec and constant m/sec. The velocity on the z (down) will depend on the tunnel upgrade or downgrade, which is about 3-5° (° means deg).

In the lateral plane of the tunnel, we present the location of the pseudolites inside the tunnel given by six squares. As you can see that there is almost symmetry[iv] (see endnote iv) in placing the pseudolites in the tunnel. For a 500-meter-long tunnel we are placing six pseudolites. Although many tunnels are longer than 0.5 km and may not be straight, these considerations can be handled during system design. It is also assumed that tunnel is 6.5m in height and is no wider than 6m. The proper location of the six pseudolites is determined after a large number of simulations. The fixed receiver is located at the center of the tunnel roof. This enables the stationary receiver to have visibility over all six of the pseudolites.

For simulation purposes we have considered several tunnel profiles, which are presented in Tab. I.

Both the moving and the stationary receivers process data at a rate of 1s per measurement. In the beginning they (the GNSS pseudolite receivers) are assumed to be perfectly synchronized with each other and with a given reference time. For simulation purposes, we assume that the 1-sigma value on the receiver pseudorange measurement noise is about 6 m, on accumulated carrier phase noise is about 3 mm, and on Doppler noise is about 1 cm/s [1]-[9].

Since the noise on the accumulated carrier phase measurement is smaller than in the pseudorange and Doppler ones; therefore, all the simulation runs presented here are obtained by processing only carrier phase measurements. Since the accumulated carrier phase implies an unknown number of integer cycles (a.k.a. as the integer ambiguity), the double difference ambiguity numbers were rounded to their closest floating-point solution. The output of the simulation is given in terms of the moving receiver position dilution of precision (PDOP) (see Fig. 8), lateral position error (dplat) (see Fig. 9), vertical position error (dpver) (see Fig. 10), lateral velocity error (dvlat) (see Fig. 11), and vertical velocity error (dvver) (see Fig. 12).

The results of the simulation runs are summarized in Tab. II.

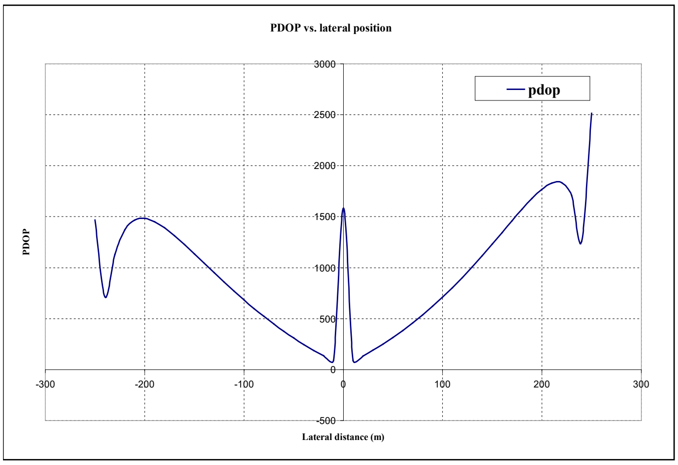

Fig. 8. Moving RCVR PDOP vs. lateral position.

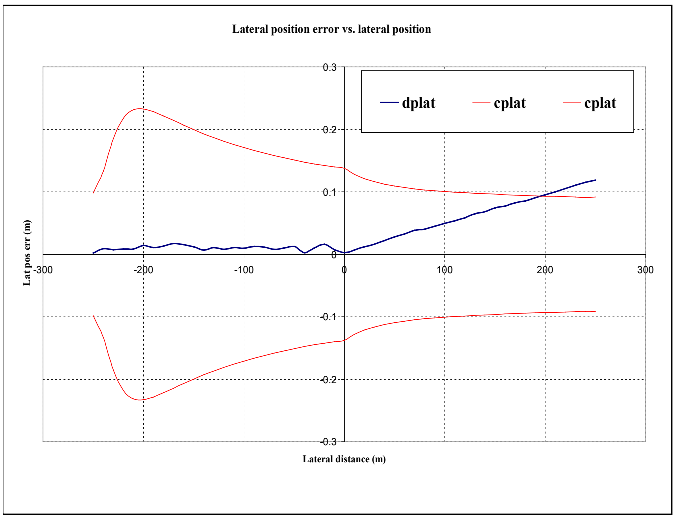

Fig. 9. Moving RCVR lateral position error vs. lateral position.

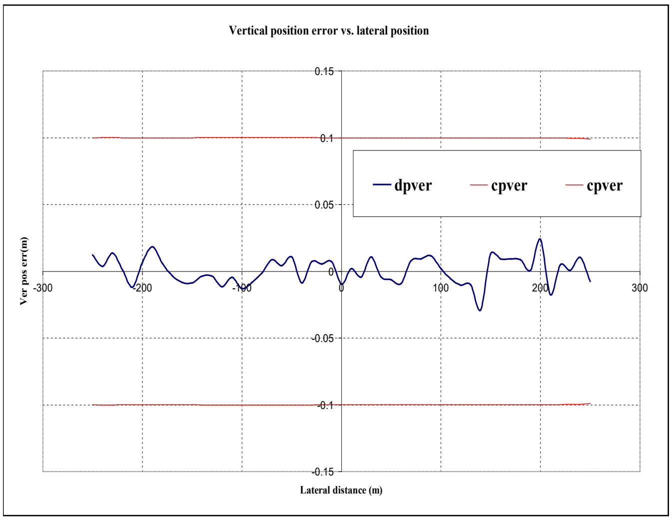

Fig. 10. Moving RCVR lateral position error vs. lateral position.

These are the sample mean and the standard deviation of the sample mean (in parenthesis) for PDOP, dplat, dpver, dvlat and dvver.

3.2 *Assessment of Simulation Results*

It appears that for straight tunnels which are up to a couple of km long, a system of three pairs of pseudolites almost (see endnote i) symmetrically positioned (see Fig. 7 and endnote iii), one receiver positioned in the center of the tunnel and another on top of the locomotive can provide lateral position and velocity accuracies of cm and cm/sec. This accuracy is maintained even when the train travels at different constant velocities.

Similar results can be obtained for tunnel trajectories with downgrade level of up to 5°.

Further investigation is required for curved tunnel profiles and for combination of both.

The implementation of this algorithm in C or C++ may be obtained via any of the algorithms discussed in [20] and in Chap. 5 of Progri, 2011, [23].

Also, it remains to perform sensitivity analysis for realistic tunnel scenarios and realistic multipath data.

This concludes the simulation and the assessment of the simulation results.

4 Conclusions

In 2000 it was significant to show that an underground system of stationary pseudolites may be used to obtain 3-D PNT or PVT by means of carrier phase double difference measurements via a Kalman filter using a simplifier multipath model [1].

The following year in 2001, we were successful to exploit other navigation algorithms such as Doppler and derived Doppler algorithms either using a system of stationary pseudolites or a combined system of GNSS satellites and stationary pseudolites [13]-[15] and further demonstrate the effectiveness of such a system even for category III precision landing in 2000 [4], and 2002 [10].

From 2002 until 2020 I was not really involved in any other work in Kalman filter design and implementation.

I believe that this work is very relevant even today because there is a number of algorithms that need to be developed and tested as a continuation of this work, which hopefully will get published soon.

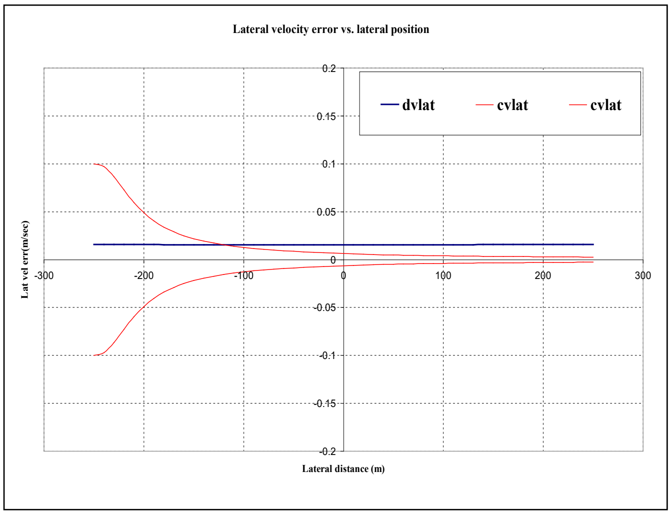

Fig. 11. Moving RCVR lateral velocity error vs. lateral position.

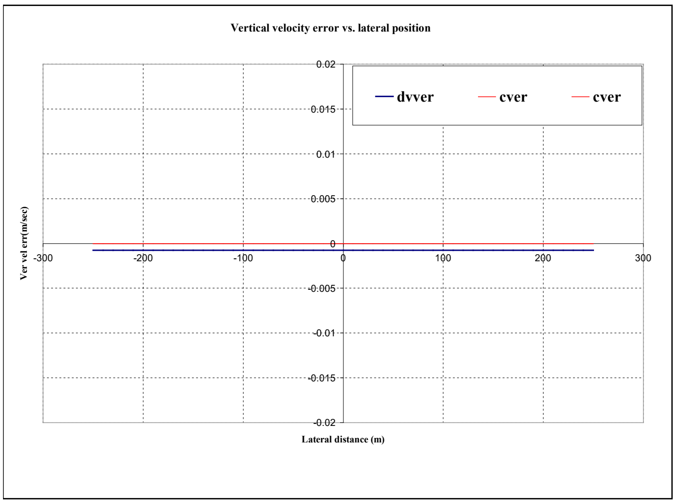

Fig. 12. Moving RCVR vertical velocity error vs. lateral position.

TABLE I: SIMULATION TUNNEL INPUT DATA

	Tunnel		Train Speed
Profile	Length (m)	Upgrade (°)	(m/s) or (km/h)
1	500	5	10(36)
2	1000	5	20(72)
3	1500	5	30(108)
4	2000	5	40(144)

TABLE II: SUMMERY OF SIMULATION RESULTS

Avr (Std)				
(PDOP)	(dplat)	(dpver)	(dvlat)	(dvver)
	(cm)		(cm/sec)	
955 (577)	4(4)	0(1)	2(0)	0(0)
3343 (1755)	3(3)	0(1)	2(0)	0(0)
7516 (4395)	4(4)	0(1)	2(0)	0(0)
14784 (11914)	3(3)	0(1)	2(0)	0(0)

5 Acknowledgement

The publication of this work in the Giftet Journal of Geolocation, Geoinformation, and Geo-intelligence was supported by Giftet Inc. executive office.

I want to profoundly thank my Ph.D. advisor Prof. William R. Michelson for his support for my Ph.D. dissertation on [22] which served as the foundation for my book on *Indoor Geolocation Systems—Theory and Applications*. *Vol. I* (Not yet available in print) [24].

6 References

[1] W.R. Michalson, I. Progri, "Assessing the accuracy of underground positioning using pseudolites," in *Proc. 13th Inter. Tech. Mtg. Sat. Div. ION (ION-GPS 2000)*, Salt Lake City, UT, pp. 1007-1015, Sep. 2000.

[2] Anon., "Least squares," *From Wikipedia, the free encyclopedia*, 2020. https://en.wikipedia.org/wiki/Least_squares

[3] J.M. Stone, J.D. Powell, "Precise positioning with GPS near obstructions by augmentation with pseudolites," in *Proc. 1996 IEEE Pos., Loc., & Nav. Sym.* (*PLANS-1996*) Palm Springs, CA, pp. 562-569, Apr. 1996. DOI: https://doi.org/10.1109/PLANS.1998.670213

[4] I. Progri, W.R. Michalson, "Performance evaluation of category III precision landing using airport pseudolites," in *Proc. 2000 IEEE Pos., Loc., & Nav. Sym.* (*PLANS-2000)*, San Diego, CA, pp. 262-269, Mar. 2000. DOI: https://doi.org/10.1109/PLANS.2000.838312

[5] A.J. Van Dierendonk, P. Fenton, C. Hegarty, "Proposed airport pseudolite signal specification for GPS precision approach local area augmentation systems," in *Proc. 10th Inter. Tech. Mtg Sat. Div. ION, ION GPS-97*, Kansas City, Missouri, pp. 1603-1612, Sep. 1997.

[6] M.G. Farley, S.G. Carlson, "Development and testing of a new pseudolite battlefield navigation system," in *Proc. 1998 Nat. Tech. Mtg. ION, Long Beach, CA*, pp. 501-509, Jan. 1998.

[7] T. Holden, T. Morley, "Pseudolite augmented DGPS for land applications," in *Proc. 10th Inter. Tech. Mtg. Sat. Div. ION (ION GPS 1997)*, Kansas City, MO, pp. 1397-1404, Sep. 1997.

[8] J., Warburton, V. Wullschleger, R. Velez, "FAA flight test results using airport pseudolites with the LAAS test prototype (LTP)," in *Proc. 10th Inter. Tech. Mtg. Sat. Div.*

ION (ION GPS 1997), Kansas City, MO, pp. 1831-1839, Sept. 1997.

[9] B. Pervan, D. Lawrence, K. Gromov, G. Opshaug, J. Christie, P.-Y. Ko, A. Mitelman, S. Pollen, P. Enge, B. Parkinson, "Flight test evaluation of a prototype local Area augmentation system architecture," in *Proc. 10th Inter. Tech. Mtg. Sat. Div. ION (ION GPS 1997)*, Kansas City, MO, pp. 1613-1621, Sep. 1997.

[10] I. Progri, W.R. Michalson, "A combined GPS satellite/pseudolite system for category III precision landing," in *Proc. IEEE PLANS 2002*, pp. 212-218, Apr. 2002. DOI: https://doi.org/10.1109/PLANS.2002.998910

[11] I.F. Progri, W.R. Michalson, J. Orr, D. Cyganski, "A system for tracking and locating emergency personnel inside buildings," in *Proc. 13th Inter. Tech. Mtg. Sat. Div. ION (ION-GPS 2000)*, Salt Lake City, UT, pp. 560-568, Sep. 2000.

[12] B.W. Parkinson, T. Stansell, R. Beard, K. Gromov, "A history of satellite navigation." *NAVIGATION*, *J. ION*, vol. 42, no. 1, pp. 109-164, 1995. DOI: https://doi.org/10.1002/j.2161-4296.1995.tb02333.x

[13] I.F. Progri, W.R. Michalson, "A navigation algorithm using a system of stationary pseudolites," *J. Geol. Geoinfo. Geointel.*, vol. 2020, article ID 2020071602, 9 pg., Nov. 2020. DOI: https://doi.org/10.18610/JG3.2020.071602

[14] I.F. Progri, J. Hill, W.R. Michalson, "A GNSS Doppler navigation algorithm," *J. Geol. Geoinfo. Geointel.*, vol. 2020, article ID 2020071603, 8 pg., Nov. 2020. DOI: https://doi.org/10.18610/JG3.2020.071603

[15] I.F. Progri, W.R. Michalson, J. Hill, "A navigation algorithm using a system of GNSS satellites and stationary pseudolites," *J. Geol. Geoinfo. Geointel.*, vol. 2020, article ID 2020071604, 8 pg., Nov. 2020. DOI: https://doi.org/10.18610/JG3.2020.071604

[16] Anon., "Integrity," *From Navipedia*, 2020. https://gssc.esa.int/navipedia/index.php/Integrity#:~:text=Integrity%20is%20the%20measure%20of,for%20navigation%20%5Bnb%201%5D

[17] B. Hofmann-Wellenhof, H. Lichtenegger, J. Collins. Chap. 8, "Mathematical models for positioning," *GPS Theory and Practice*. 5nd Ed., Wien, Austria: Springer-Verlag, 382 pg., 2001.

[18] B.S. Pervan, C.E. Cohen, B.W. Parkinson, "Integrity monitoring for precision approach using kinematic GPS and a ground-based pseudolite," *Navigation*, vol. 41, no. 2, pp. 159-174, summer 1994. DOI: https://doi.org/10.1002/j.2161-4296.1994.tb02569.x

[19] K. Pahlavan, A.H. Levesque, *Wireless Information Networks*. New York, NY: John Wiley & Sons, Inc, 1995, pp 42.

[20] W.H. Press, S.A. Teukolsky, B.P. Flannery, W.T. Vetterling, *Numerical Recipes in C, The art of scientific Computing*. 2nd Ed., New York, NY: Cambridge University Press, 1992.

[21] R.G. Brown, P.Y.C. Hwang. *Introduction to Random Signals and Applied Kalman Filtering*. New York, NY: John Wiley & Sons, Inc. 1997.

[22] I. Progri, "An assessment of indoor geolocation systems," *Ph.D. Dissertation*, Worcester Polytechnic Institute, 408 pg., May 2003.

[23] I. Progri, *Geolocation of RF Signals—Principles and Simulations*. 1st ed., New York, NY: Springer Science & Business Media, LLC, 330 pg., Jan. 2011. DOI: https://doi.org/10.1007/978-1-4419-7952-0

[24] I. Progri, *Indoor Geolocation Systems—Theory and Applications*. *I*, 1st ed., Worcester, MA: Giftet Inc., ~800 pp., ~ 2020 (not yet available in print).

---

i *Editor's Note*: This article was originally published in 2000 [1]. The main results of this article are valid if only the data are assumed to be normally or Gaussian distributed [21]. For other types of data distributions, I believe that a modification of the algorithm may be needed. The original publication contained a few typos and some minor language problems that I believe are fixed in this edition. A number of other clarifications are made in this publication and also the equation editor is greatly improved. Since, the original article did not contain a DOI and it is a copyright by the authors I believe that the publication of this article in the form of a technical report is a good way to preserve the originality and authenticity of the article and provide a much.

ii Cutaway is a diagram or drawing with some external parts left out to reveal the interior.

iii Regarding this issue Pahlavan, Levesque (1995, pg. 42 [17]) writes "Except for the LOS path, all paths are going through at least one order of reflection, transmission, or diffraction before arriving at the receiver. At this stage let us consider only the reflections. Upon each reflection of a path from a surface, a certain fraction of the power is absorbed by the surface, and the remainder of the power in that path carries beyond the reflection."

iv Due to the symmetry of the problem, the distance $d_{m-i}^{j-l}[k]$ is equal to zero; therefore, this solution is associated with a severe observability problem. In order to avoid this singularity, we will placed pseudolites at locations slightly different which will result in $d_{m-i}^{j-l}[k]$ different from zero at the same time mitigating the multipath effect.